Siamese Distinguishing Features Attentional Enhancement Transfer Fault Diagnosis Method for Variable Rotational Speed

KUN XU[1,2], SHUNMING LI[1], RANRAN LI[1], JIANTAO LU[1], and MENGJIE ZENG[1]

[1]College of Energy and Power Engineering, Nanjing University of Aeronautics and Astronautics, Nanjing 210016, China
[2]School of Computer Science and Engineering, Nanyang Technological University, SG 639778, Singapore

Corresponding author: Jiantao Lu (e-mail: lujt@nuaa.edu.cn).

ABSTRACT Transfer learning is widely used in artificial intelligence fault diagnosis field because it can solve the problem of label missing in rotating parts at varying speeds. However, the domain adaptive method in transfer learning is not suitable for real transfer fault diagnosis scenarios, and the adaptive enhancement of fault characteristics is not realized in the transfer process. To solve these thorny problems, a novel method called Siamese Distinguishing features Attentional Enhancement Transfer fault diagnosis (SDAET) has been proposed. The body of SDAET model adopts the dual-branch convolutional neural network architecture with shared weights. It mainly uses the contrast loss function in the siamese feature contrast network to extract the domain invariant features at two rotational speeds, and then applies it to the transfer diagnosis at other rotational speeds, so as to meet the more real transfer diagnosis scenarios. The distinguishing features attentional enhancement network is designed to adaptively enhance the differentiated domain invariant features at different rotational speeds. Furthermore, various feature visualization techniques are used to further explain the features learned from the black box neural network. The diagnostic results on two kinds of test datasets show that the proposed model has higher diagnostic accuracy. The technique of siamese distinguishing features attentional enhancement provides a new and better way to solve the transfer diagnosis problem.

INDEX TERMS Artificial intelligence, fault diagnosis, siamese, attentional enhancement.

I. INTRODUCTION

The era of industrial Internet puts forward higher requirements for the health management and intelligent operation and maintenance of equipment[1, 2]. A large number of traditional signal processing based methods have been widely used in equipment health monitoring and maintenance management [3, 4]. For example, Fourier transform, wavelet transform, spectral kurtosis, empirical mode decomposition, variational mode decomposition and so on [5]. All kinds of signal processing methods have played a good effect on the health diagnosis and maintenance of equipment. However, the fly in the ointment is that the signal processing method requires a lot of prior knowledge and manpower [6]. With the rise of deep learning, it is gradually applied to solve the problem of online intelligent fault diagnosis because it can intelligently extract fault features and classify them [7].

At the beginning, intelligent fault diagnosis mainly focused on how to intelligently extract and classify signal features [8, 9]. A large number of scholars have conducted relevant researches, and excellent diagnosis results have been achieved in a single working condition [10, 11]. Nowadays, the difficult problems of intelligent diagnosis have gradually started to focus on the fault diagnosis in variable speed [12], unbalanced sample [13] and noise environment [14]. As the problem of variable speed transfer diagnosis is a basic problem to be solved in almost all equipment, transfer fault diagnosis [15, 16] has become a hot research topic at present.

For the transfer fault diagnosis under variable speed or working conditions, according to the different method types,

it can be divided into three categories: difference-based approach [17], adversarial-based approach [18], refactor-based approach [19] and others, as shown in Figure 1.

The difference-based approach mainly adopts the idea that the untagged target domain data also follows the tagged source domain data for common training. Then various feature alignment methods are used in the high-dimensional space to align the differentiated distribution features of the source domain and the target domain so as to realize the transfer diagnosis of the target domain [20]. For example, Yang et al.[21] innovatively proposed a polynomial kernel induced maximum mean discrepancy method to extract domain invariant features, thus realizing transfer diagnosis. Li et al. [22] presented a domain adaptive method for feature alignment in high dimensional space using central moment discrepancy. Qian et al.[23] proposed a domain adaptive method based on coral loss alignment to extract domain invariant features.

The main ideas of adversarial-based approach adoption are similar to those of difference-based approach adoption. The difference lies in that this method mainly adopts adaptive learning technology to align the features of source domain and target domain in high dimensional space [24]. For instance, Jiao et al.[25] presented a residual joint adversarial network from adaptive alignment of domain invariant features in high dimensional space to realize transfer diagnosis at variable rotational speeds. Chen et al. [26] proposed a novel domain adversarial transfer network to intelligently align the features in high dimensional space.

Although the above two kinds of transfer diagnosis methods have achieved high transfer diagnosis accuracy, they still have their shortcomings in practical application. It can be seen from the above description that the two kinds of method needs to assume that the type of target domain fault samples at another rotational speed is the same as that of the source domain fault samples. In addition, in order to diagnose the target domain samples at another rotational speed, the model must be trained again. These assumptions limit the application of the transfer model in the actual diagnosis for variable speed faults.

The main idea of the reconstruction-based approach [27] is to restore the sample of the target domain as much as possible with the decoder. Gu et al. [28] innovatively input the reconstructed signals into the neural network through the symmetric point mode to realize the transfer diagnosis of bearing faults under variable working conditions.

Of course, there are other kinds of intelligent transfer diagnosis algorithms. Zhang et al. [29] innovatively proposed a limited data rolling bearing fault diagnosis method based on siamese networks. This work solves the problem of variable speed, ambient noise and small sample size almost simultaneously, which is very remarkable research. Li et al. [30] introduced the attention mechanism to assist the deep network to locate information data segments, and realized the intelligent diagnosis with small samples.
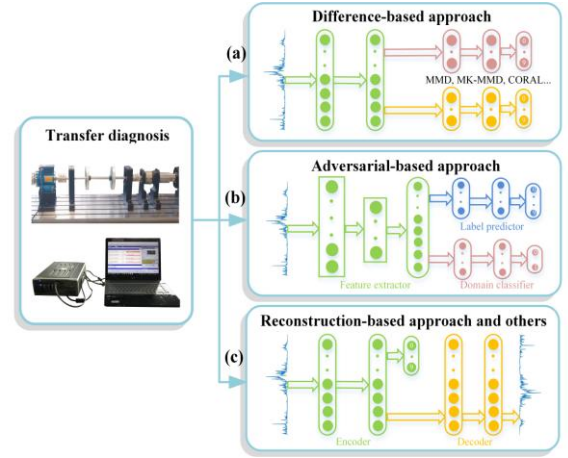

FIGURE 1. Transfer fault diagnosis classification. (a) Difference-based approach; (b) Adversarial-based approach; (c) Reconstruction-based approach and others.

However, firstly, it can be seen from the above analysis that we need a transfer diagnosis model that can better meet the actual variable speed application scenarios. Target domain samples do not need to follow source domain samples for joint training to complete the transfer diagnosis for target domain samples; Secondly, it is better that the transfer model can extract as much as possible the domain invariant features at two rotational speeds during the training process, and then it can be used for transfer diagnosis at other rotational speeds. At the same time, it is better for the model to adaptively enhance the distinguishing domain invariant features at the two rotational speeds during training; Finally, we also need more feature visualization techniques to explain the black box of neural network, so as to find the connection between the features learned by deep learning model and the fault features in physical practice. In order to realize the above three points, we have made our own efforts.

In this paper, we propose a new method called Siamese Distinguishing features Attentional Enhancement Transfer fault diagnosis (SDAET) to address these thorny issues. The main innovation contributions of this paper can be summarized as follows:

(1) A model called Siamese Distinguishing features Attentional Enhancement Transfer fault diagnosis (SDAET), which can be used to train at two speeds at the same time and test the another speed, is proposed. And the model is more suitable for real transfer fault diagnosis scenarios.

(2) Novel distinguishing features attentional enhancement (DFAE) network is employed to reasonably enhance the differentiated domain invariant characteristics at the two rotational speeds and achieve better diagnostic classification results.

(3) The novel feature visualization technology visualizes the relationship between the features extracted by the neural network and the input signal, which better explains the black box of deep learning, which also provides a visualization idea for other intelligent diagnosis methods.

The rest of the paper is organized as follows: The second part is background, and the third section focuses on describing our proposed approach. Section IV focuses on the results achieved by the model and the various feature visualization results. The fifth part verifies the model on private datasets. The last section is the conclusion.

II. KNOWLEDGE BACKGROUND

The inspiration for convolutional neural network algorithms originated from human research on animal visual systems. Its main modules include convolution layer, pooling layer, full connection layer and classification layer. Assuming W represents the weight, b represents the bias, y is the output result after convolution, and z is the result after activation, then the expression of convolution activation can be expressed as:

$$y_j(i) = W_j * x(i) + b_j \tag{1}$$

$$z_j(i) = relu[y_j(i)] = \max[0, W_j * x(i) + b_j] \tag{2}$$

It is proved that the batch normalization [31] can reduce the overfitting and replace the regularization parameters to a certain extent, and has good network performance. We add it after the convolution layer activation function. Assuming that E represents the mean value and Var denotes the variance, the process of batch normalization can be expressed as follows:

$$E[x_\varphi] = \frac{1}{m} \sum_{j=1}^{m} x_j \tag{3}$$

$$Var[x_\varphi] = \frac{1}{m} \sum_{j=1}^{m} (x_j - E[x_\varphi])^2 \tag{4}$$

$$\hat{x}_j = \frac{x_j - E[x_\varphi]}{\sqrt{Var[x_\varphi] + \varepsilon}} \tag{5}$$

$$\hat{y}_j = \gamma \hat{x}_j + \beta \tag{6}$$

where x_φ represents the batch data and ε denotes a small positive number used to avoid divisors of 0. γ represents the scale factor and β denotes the translation factor. These two parameters are self-learned by the network during training.

In order to further reduce the training parameters in model training, a pool layer is tried to select features. Maximum pooling is adopted to retain peak characteristics in the training process of the model as much as possible. Its function is as follows:

$$p_j(i) = \max_{field}[\hat{y}_j(i)] \tag{7}$$

where p represents the pooling feature, and $field$ is the pooling area.

The global average pooling layer is also placed after the last convolution layer to minimize the parameters of the model. The formula is as follows:

$$p_{gap}(i) = \underset{field}{Average}[z_j(i)] \tag{8}$$

At the end of the model is a full connection layer and the softmax activation function.
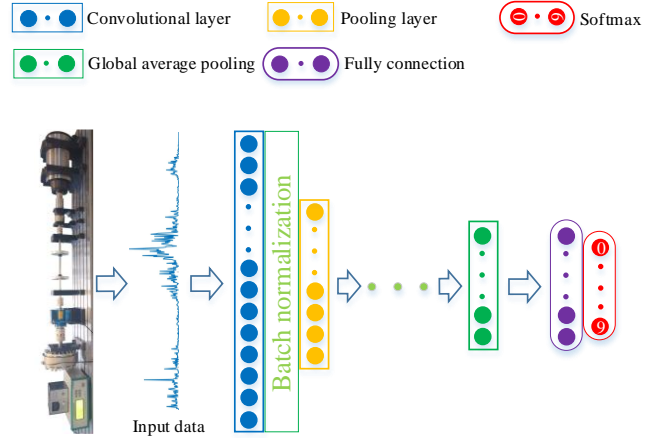

FIGURE 2. Schematic diagram of convolutional neural networks using batch normalization and globally average pooling layer.

The SDAET model proposed in this paper adopts the above knowledge theory in the infrastructure, and the schematic diagram of the infrastructure is shown in Figure 2.

III. DIAGNOSIS METHOD

In order to better adapt to the transfer diagnosis scene, and adaptively enhance the local features to improve the diagnosis accuracy, we proposed the Siamese Distinguishing features Attentional Enhancement Transfer (SDAET) model. The model mainly uses the data of any two rotational speeds as the training data to train the model, so that the trained model can be directly applied to the transfer diagnosis of other rotational speeds. The main framework of the SDAET model is a dual-branch convolutional neural network system with shared weights, which mainly includes the distinguishing features attention enhancement network, siamese feature contrast network and feature classification network. The architecture diagram is shown in Figure 3.

The distinguishing features attention enhancement (DFAE) network is placed after the fifth convolutional layer and its main purpose is to enhance the features extracted from the model. The Siamese feature contrast network is placed on the global average pooling layer. Its main purpose is to compare two rotational speed domain invariant features to make them as similar as possible. At the same time, the reason why it follows after the DFAE is also for the convenience of cooperating with the feature enhancement network to jointly extract the distinguishing domain invariant features at two rotational speeds. The detailed parameters of the model are shown in Table I. Next, we explain in detail the three main networks used in the model.

A. FEATURE CLASSIFICATION NETWORK

The main purpose of feature classification network is to use supervised learning method to classify the input data correctly. In this paper, softmax activation function is mainly used to classify data. The formula is as follows:
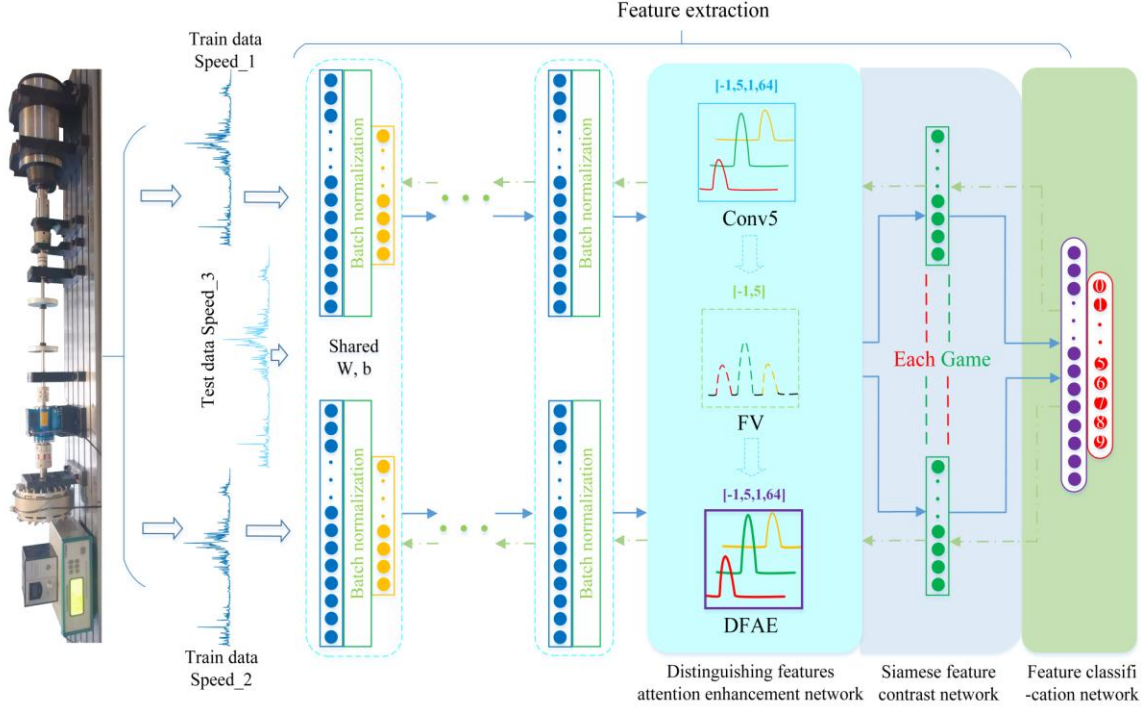
FIGURE 3. Network architecture of the SDAET model.

$$q(z_j) = e^{z_j} / \sum_k^C e^{z_k} \qquad (9)$$

Where q represents the probability of classification and C represents the total number of categories.

Cross entropy loss function is used to calculate the loss of feature classification network during training. Its mathematical expression is as follows:

$$L_{class} = -\sum_z \{p(z) \log q(z) + [1 - p(z)] \log[1 - q(z)]\} \quad (10)$$

where p denotes the correct classification of sample labels.

Under the constraint of supervised cross-entropy loss function with labels, the input data and label content are correctly matched and classified.

B. FEATURE ENHANCEMENT NETWORK

The function of distinguishing features attentional enhancement (DFAE) network is to adaptively enhance the features in the process of network learning, so as to improve the diagnosis accuracy[32]. The DFAE is placed after the last convolution layer, which mainly includes feature visualization (FV) module and distinguishing features attentional enhancement (DFAE) module.

The purpose of FV module is to visualize the features after the convolution layer. Its basic idea is to sum and accumulate the features of each channel for the convolution layer, so as

to visualize the attention segment with higher feature values. The length of the feature fragment output by the last convolution layer 5 is *[5,1]*, and the number of channels is 64. We sum and accumulate its features in the channel dimension, and the calculation diagram is shown in Figure 4. The formula for the first step is as follows:

$$z_{j,M}(i) = \sum_{channels|_{m=1}^{M=64}} z_{j,m}(i) \qquad (11)$$

where M denotes the total number of channels and m is the channel. j represents for attention segment.

TABLE I
THE SDAET DETAILS PARAMETERS

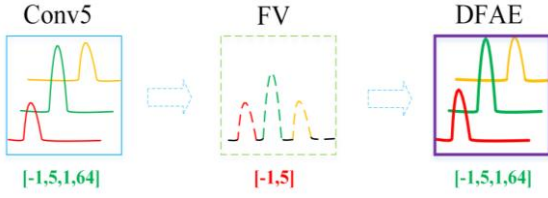| No.	Layer	Kernel Size/Stride	Channel Size	Output Zize	Padding
1	Conv1	15*1/3*1	16	200*16	Yes
2	Pool1	2*1/2*1	16	100*16	Yes
3	Conv2	15*1/3*1	32	34*32	Yes
4	Pool2	2*1/2*1	32	17*32	Yes
5	Conv3	3*1/1*1	48	17*48	Yes
6	Pool3	2*1/2*1	48	9*48	Yes
7	Conv4	3*1/1*1	64	9*64	Yes
8	Pool4	2*1/2*1	64	5*64	Yes
9	Conv5	3*1/1*1	64	5*64	Yes
10	DFAE	5*1	64	5*64	/
11	GAP	/	64	64	/
12	Fc1	64	/	10	/
13	Softmax	/	/	10	/

FIGURE 4. Diagram of distinguishing features attention enhancement (DFAE) network.

As can be seen from Table I, after calculation by the above formula, the output dimension in the training process changes from the original *[-1,5,1,64]* to *[-1,5,1]*. In order to activate it using the attentional mechanism, we convert its dimension to *[-1,5]*. The *-1* represents each batch of samples, and *5* denotes five characteristic attention segments, assumed to be labeled A_1 to A_5. The attention activation function adopts softmax activation function, and the final attention value output by FV is:

$$FV = Attention = [A_1, A_2, A_3, A_4, A_5]_{samples}$$

$$= softmax[z_{j,M}(i)] + 1 = e^{z_{j,m}(i)} \Big/ \sum_{i=1}^{J=5} z_{j,m}(i) \quad (12)$$

Note that in the formula above, in addition to using the activation function to activate the attention segment, it is also increased by **1**. This is because the value output by the softmax activation function must be in the range 0 to 1. And if we use the values in this range as the weight matrix to enhance the features, it will actually decrease the corresponding features. However, when we add **1** to it, the value range of attention weight becomes from 1 to 2, which can be used as the weight matrix to enhance attention features.

FV module can be used to calculate the weight matrix of enhanced attention features, and visualization of the weight matrix can also reveal the attention segment that the model mainly pays attention to during the training process. The output of the DFAE module is obtained by multiplying the obtained weight matrix with the original feature fragments. The calculation formula is as follows:

$$DFAE = z_{j,m}(i) * FV$$

$$= z_{j,m}(i) * [A_1, A_2, A_3, A_4, A_5]_{samples} \quad (13)$$

According to the above calculation formula, as shown in Figure 4, the final output feature dimension of DFAE module is changed to the original *[-1,5,1,64]*. It can be seen from the calculation process formula that the features of some attention segments are enhanced.

In combination with the siamese network, DFAE network can enhance the distinguishing domain invariance features of the two input data respectively. Next, we will introduce the siamese feature contrast network.

C. SIAMESE FEATURE CONTRAST NETWORK
The idea of siamese networks [33] comes from the game theory, which compares the difference between features by

contrast loss functions. By adding a siamese feature contrast function to the global average pooling layer of the two-branching CNN structure, the domain invariant features from the two data are aligned. Moreover, it works with the DFAE network, and the final results show that the model extracts the differentiated domain invariant features from the two types of data.

The label of the siamese network is determined by the label of the two sets of source domain data. If the labels for data from both source domains are the same, it is 1; if they are different, it is 0. The physical meaning of contrast loss function in the model is to compare the similarity of features from two kinds of data in high dimensional space. If they are similar, the value of loss function is 0; if they are not similar, its value is positive. It is assumed that gap_1 and gap_2 respectively represent the characteristics of the data from the two rotational speeds in the high-dimensional space, and SM represents the matrix similarity measure.

$$L_{siamese}(l, gap_1, gap_2) = (1-l)L_G(SM) + lL_I(SM)$$

$$= (1-l)\frac{2}{Q}(SM)^2 + (l)2Qe^{\frac{-2.77}{Q}SM} \quad (14)$$

Where l indicates whether the true feature labels of the two global average pooling layers are the same. L_G denotes the loss when the two types of data features come from the same category, and L_I is the loss when the two types of data features come from different categories.

Then, according to the description of siamese network literature [33] and the specific application scenario in this paper, the above formula can be rewritten as:

$$L_{siamese} = \frac{1}{n}\sum_{i=1}^{N}\left\{ \begin{array}{l} (1-l^i)\frac{2}{Q}[SM(gap_1^i, gap_2^i)]^2 \\ +2l^iQe^{\frac{-2.77}{Q}SM(gap_1^i, gap_2^i)} \end{array} \right\} \quad (15)$$

Assuming d represents the dimension of global average pooling layer features, then the matrix similarity measure SM can be expressed as:

$$SM(gap_1, gap_2) = \frac{1}{d} \| gap_1 - gap_2 \|_2 \quad (16)$$

It can be seen from the above description that the siamese feature contrast network extracts domain invariant features by making the features from the two types of data play games with each other in the high-dimensional space.

D. TOTAL LOSS
The SDAET model is mainly composed of the above network, and its total loss mainly includes two parts, which can be written in the following form:

$$L_{num} = L_{class} + \mu L_{siamese} \quad (17)$$

In the above equation, μ represents the penalty coefficient, which decreases gradually as the number of training steps increases. This is mainly to prevent the comparison loss value from greatly affecting the training results at the end of

model training. Assuming *st* is the training progress linearly changing from 0 to 1. Then its expression can be written as:

$$\mu = \frac{2}{1+\exp(-10 \times st)} - 1 \tag{18}$$

Adam random gradient descent algorithm [34] was adopted in the process of model training, the learning rate was set to 0.001, the batch size was set to 100, and the total number of iterative steps was 1000. Following the gradient descent algorithm, the total loss can be expressed as follows:

$$L_{num} = \min_{Adam}(L_{class} + \mu L_{siamese}) \tag{19}$$

It can also be seen from the above total loss function that the SDAET model proposed by us is not complex, which may be more suitable for simple applications in practical diagnosis.

IV. VERIFICATION ON OPEN DATASET

Case Western Reserve University's Bearing Health Monitoring dataset [35] is an accepted standard dataset. We first use this dataset to verify the performance of the proposed algorithm. The test rig consists of a 1.5kW induction motor, torque sensor, acceleration sensor and indicator. The specific model of the experimental bearing is SKF6205, which is installed on the bearing base. We mainly used the bearing monitoring signal near the motor driving end, and the data sampling frequency was 12kHz. The health status of bearings is mainly divided into four categories, namely: normal condition, fault in roller, fault in inner race and fault in outer race. For the three types of fault bearings, each fault type can be subdivided into three different fault depths, which are crack depths of 0.007 inches, 0.014 inches, and 0.021 inches. Their overall health can then be divided into ten types, described in detail in Table II.

TABLE II
OVERALL HEALTH DESCRIPTION

Fault types	Nor	Fault in roller			Fault in inner race			Fault in outer race		
Severity (10⁻³inc)	0	7	14	21	7	14	21	7	14	21
Category	C0	C1	C2	C3	C4	C5	C6	C7	C8	C9

The data of the above ten types of health conditions were mainly obtained at the following four different load speeds: 1730r/min, 1750r/min, 1772r/min and 1797r/min (A, B, C and D). In order to fully test the performance of the model and visualize the feature correlation between the features learned by the model and the physical actual meaning as much as possible, we use unnormalized frequency domain data as signal input. The sample size for each health condition was 1000 and the data length was 600. Therefore, for example, for the dataset at speed A, the total dataset size is [10000, 600].

In order to test the validity of the model to the maximum extent, we compare the proposed model with mainstream transfer learning models and transfer learning methods. The comparison models mainly include WDCNN model [14] which has been proved to have high transfer performance, MMDCNN model which has SDAET basic framework and uses MMD transfer algorithm [36], and SiaCNN model which is the SDAET model after removing DFAE module. The transfer diagnosis comparison between them is shown in Figure 5

As can be seen from Figure 5, compared with other mainstream transfer models, the proposed SDAET model achieves the highest average transfer diagnosis performance, with the average transfer accuracy reaching 97.67%. For the
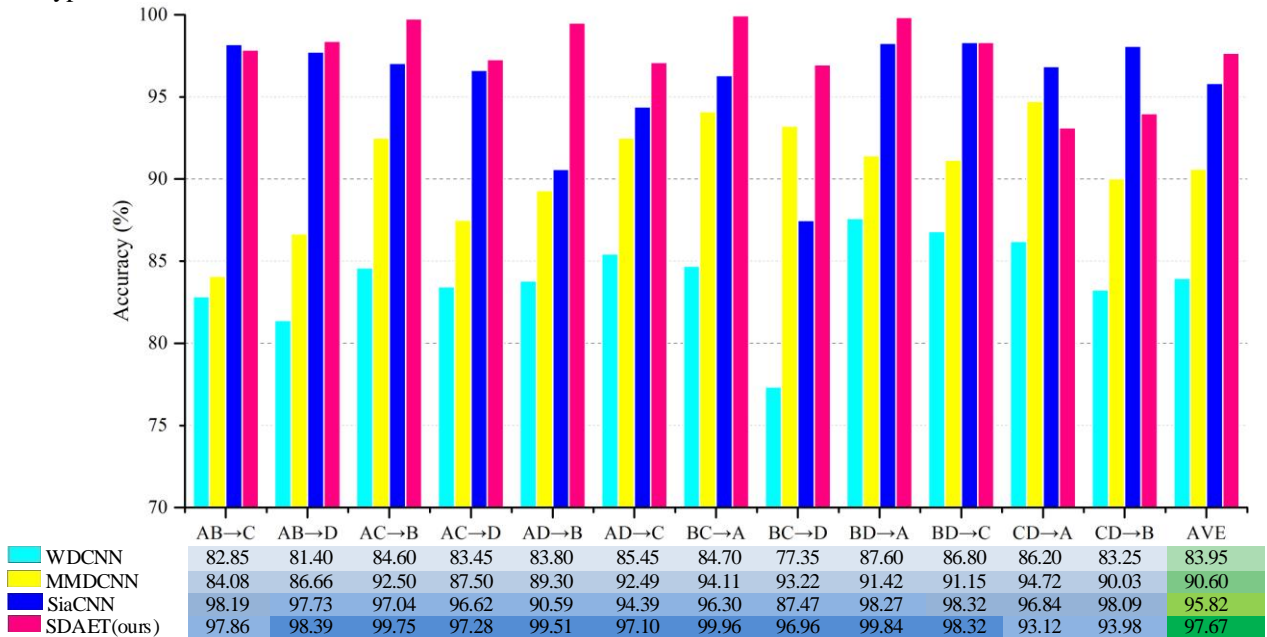

	AB→C	AB→D	AC→B	AC→D	AD→B	AD→C	BC→A	BC→D	BD→A	BD→C	CD→A	CD→B	AVE
WDCNN	82.85	81.40	84.60	83.45	83.80	85.45	84.70	77.35	87.60	86.80	86.20	83.25	83.95
MMDCNN	84.08	86.66	92.50	87.50	89.30	92.49	94.11	93.22	91.42	91.15	94.72	90.03	90.60
SiaCNN	98.19	97.73	97.04	96.62	90.59	94.39	96.30	87.47	98.27	98.32	96.84	98.09	95.82
SDAET(ours)	97.86	98.39	99.75	97.28	99.51	97.10	99.96	96.96	99.84	98.32	93.12	93.98	97.67

FIGURE 5. Transfer diagnosis results of the proposed SDAET model and comparison models under different working conditions.
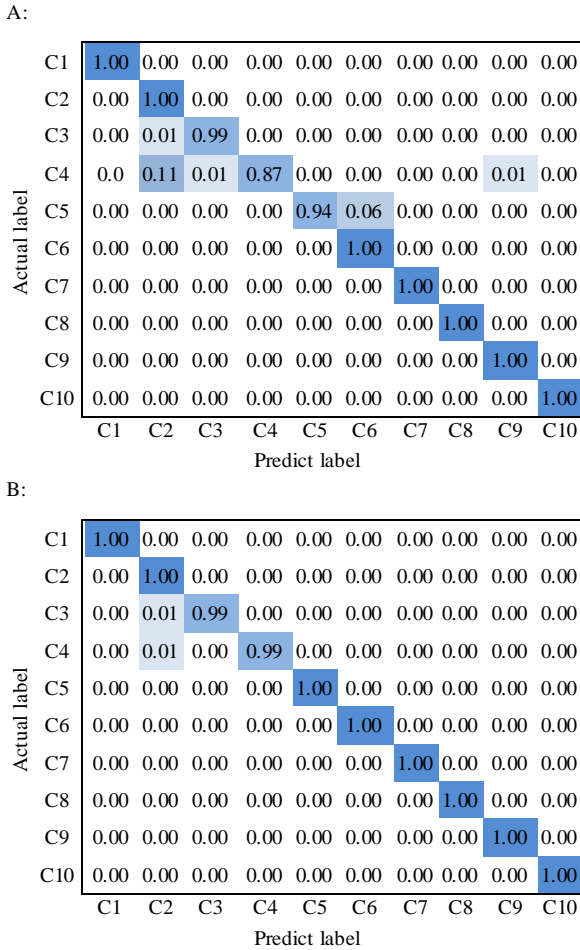
A:

B:

FIGURE 6. Confusion matrix for transfer diagnosis in the condition of AD→B. (A) SiaCNN model. (B) SDAET model.

SiaCNN model, that is, the SDAET model excluding the DFAE network and only including the siamese feature contrast network achieves a relatively high diagnostic performance, with the average accuracy of migration diagnosis reaching 95.82%, which is second only to the proposed model. This also proves the effectiveness of our proposed DFAE network. The MMDCNN model with good MMD transfer learning algorithm only achieves an average of 90.06% transfer diagnosis performance. The performance of WDCNN with only a certain domain adaptive ability is relatively the least ideal. These illustrate the excellent performance of our proposed SDAET model in a more comparative way.

In order to further demonstrate the diagnostic results of the models, we plotted the transfer diagnostic confusion matrices of the two models under the same working condition, as shown in Figure 6. From the confusion matrix, it can be seen that although the SiaCNN model has relatively good migration performance, it produces large misclassification for some fault types, such as fault in roller. In contrast, our proposed model achieves excellent classification performance for each health condition. In order to show the

causes of the above phenomena in more detail and to further illustrate the effectiveness of the DFAE network, we draw the contrast of enhanced attention features at the DFAE layer, as shown in Figure 7.

In Figure 7, A and B are respectively the expanded visual results of the features of fault types C3 and C5 in the fifth convolution layer and DFAE layer. It can be seen from the circled places in the figure that after the features pass through the DFAE layer, their absolute values become larger, that is, they are enhanced. In addition, it can be seen from the overall feature trend diagram that although the features have been enhanced to a certain extent, the overall variation trend of the features has not changed. The enhanced features enable the model to achieve better classification results. This is why the two models in Figure 6 produce different transfer diagnostic performance.
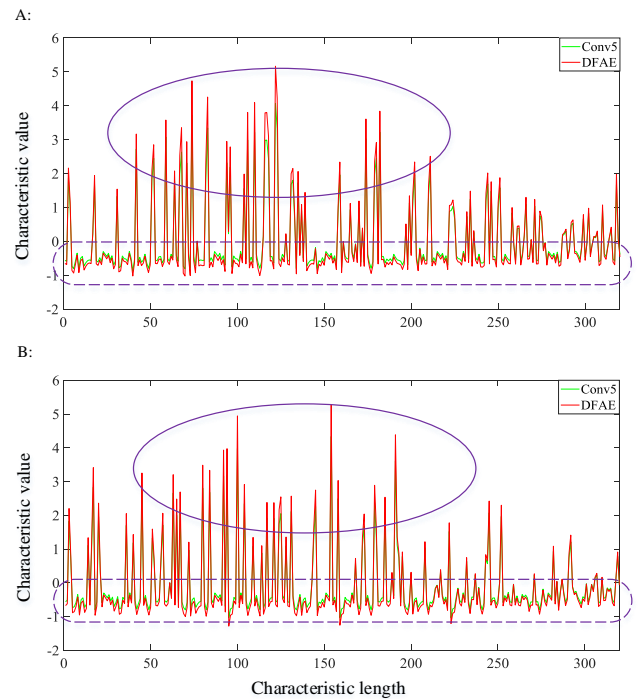
A:

B:

FIGURE 7. Visualization results of enhanced attention features in DFAE layer. (A) Fault types C4. (B) Fault types C5.

In order to verify that the proposed model extracts the differentiated enhanced domain-invariant features at two rotational speeds, we use the FV module to visualize the feature attention of the FV layer, as shown in Figure 8. We observed from Figure 8 that the model extracted distinguishing enhancement domain invariant features, because the feature attention segments at two rotational speeds were different in the figure. This confirms that the SDAET model achieves a relatively high transfer performance due to the distinguishing enhanced domain invariant features at two different rotational speeds extracted by DFAE module. This also proves the effectiveness of the DFAE module.
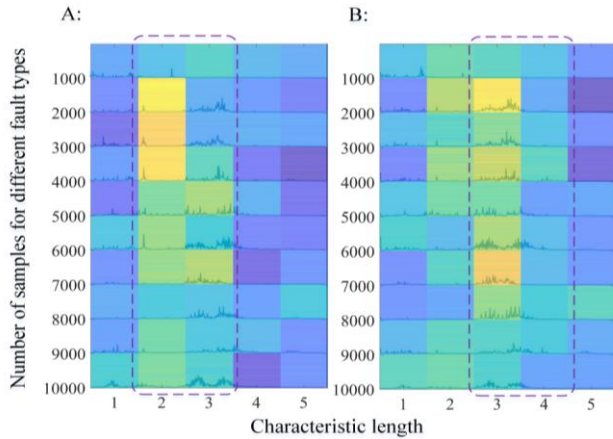
FIGURE 8. Characteristic attention segments at two different rotational speeds during training. (A) Speed A. (B) Speed D.

The effectiveness of the siamese feature contrast network is verified by another kind of feature visualization method. We visualized the characteristics of the global average pooling layer at two rotational speeds, and compared the SDAET model and SiaCNN model. The visualized images are shown in Figure 9 and Figure 10, respectively. As can be seen from Figure 9, the features extracted by the SDAET model without the siamese feature contrast network are not obvious enough, especially for the feature extraction at another rotational speed.

As can be seen from the feature visualization results in Figure 10, the proposed SDAET model has a good classification of features at both speeds, and more importantly, the features at the two speeds are almost similar. This further proves that the proposed model can extract the distinguishing domain invariant features at two rotational speeds in the global average pooling layer, and also further supports the effectiveness of the siamese feature contrast network.

Finally, in order to further demonstrate the effectiveness of the twin comparison network, we use the T-SNE feature visualization method to draw the feature map. The comparison and display results of the two models in the global average pooling layer are shown in Figure 11. It can
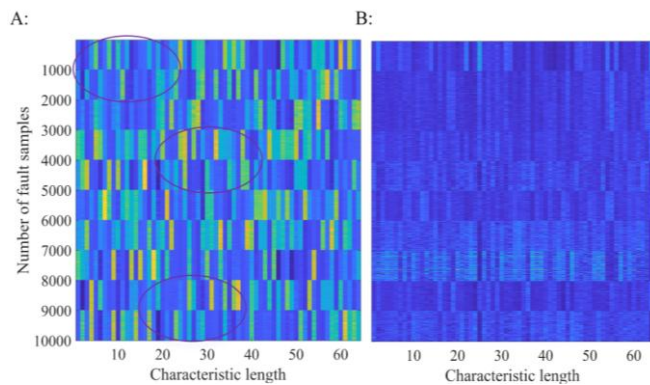

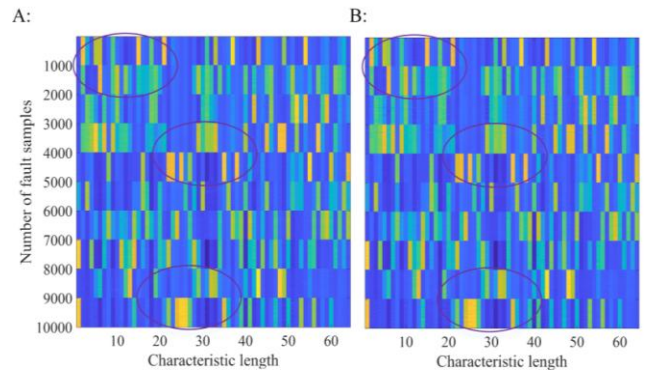FIGURE 9. The SDAET model without Siamese feature contrast network. (A) Speed A. (B) Speed D.

FIGURE 10. The proposed SDAET model. (A) Speed A. (B) Speed D.

be observed from the figure that the SDAET model without siamese feature contrast network has poor classification results at two rotational speeds, and many features are stacked together, as shown in Figure 11(A). As can be seen from Figure 11(B), the proposed model achieves excellent classification effect, and the fault types at each speed are clearly separable, which further proves the excellent performance of the SDAET model.
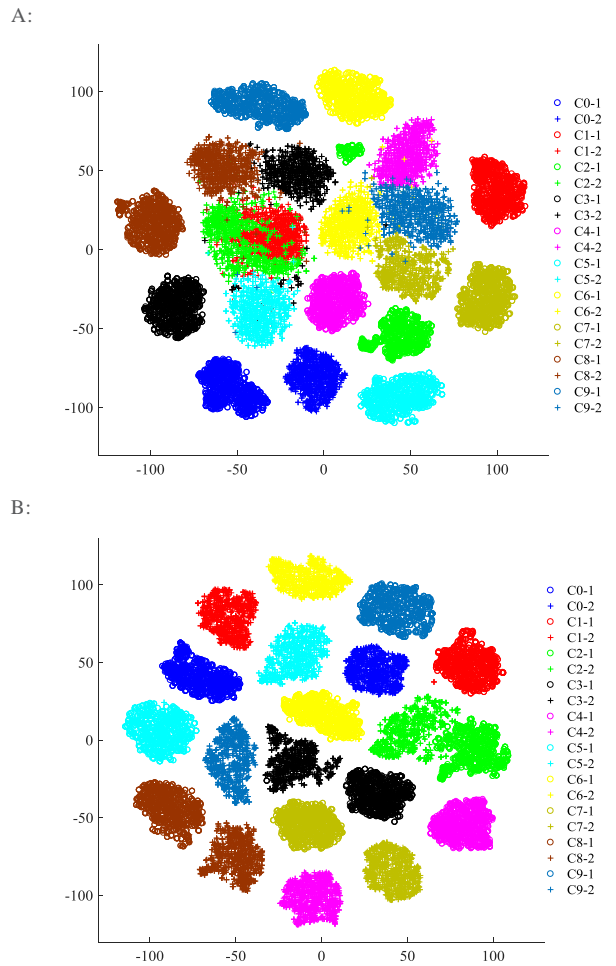

FIGURE 11. Feature visualization via t-SNE in globally average pooling layer. (A) The SDAET model without Siamese feature contrast network. (B) The proposed SDAET model.

V. VERIFICATION ON PRIVATE DATASET

Private dataset from a fault diagnosis test bench are further used to verify the performance of the proposed model. The fault diagnosis test bench and faulty components are shown in Figure 12. The test bed mainly includes a motor, a transmission belt, a coupling, a rotor, a bearing and a bearing base. The vibration acceleration sensor is vertically mounted on the bearing base. The specific model of cylindrical roller bearing is NU205EM. As shown in Figure 12(B), three main fault types are set. The depth of each fault type is 0.5mm, and the detailed classification is shown in Table III. The sampling frequency is 25.6kHz.
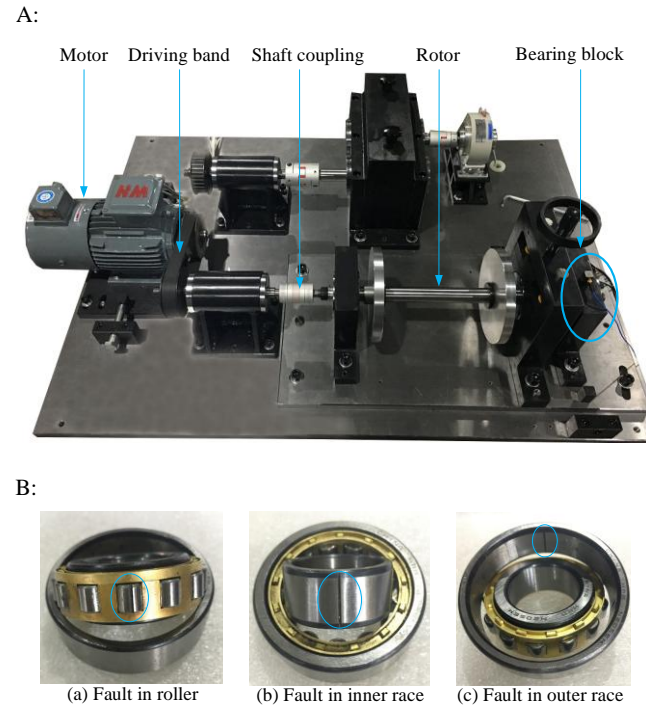
TABLE III
OVERALL HEALTH DESCRIPTION

Fault types	Nor	Fault in roller	Fault in inner race	Fault in outer race
Severity (mm)	0	0.5	0.5	0.5
Category	C0	C1	C2	C3

A:

B:

FIGURE 12. **(A) Fault diagnosis test bench. (B) The fault components.**
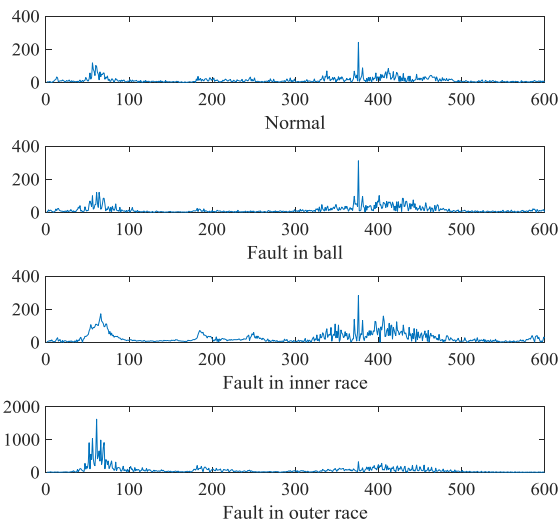
FIGURE 13. **Spectrum of different health conditions.**

We have collected four kinds of data with relatively large span of rotation speed, which are 1000r/min, 1100r/min, 1300r/min and 1500r/min (A, B, C and D) respectively. The longer the rotation speed variation span, the more difficult it should theoretically be to achieve good transfer diagnosis results. We mainly compared the proposed SDAET model with WDCNN [14] and WAFCNN [32], which have been proved to have better transfer diagnosis performance. For the model that could not be trained with two kinds of rotational speed data input at the same time, the average diagnostic accuracy of migration at two kinds of rotational speed was taken as the comparison result.

We draw the results of multiple transfer experiments of the proposed SDAET model and the comparison model under transfer conditions AC to B, as shown in Figure 14. As can be seen from the figure, our proposed SDAET model still achieves a very high accuracy of transfer diagnosis, reaching an amazing accuracy of about 98.5% even under a large rotational speed span. In addition, it can be seen from the results of ten migrations that the proposed model also has good diagnostic stability. However, the transfer results obtained by the two mainstream models with domain adaptive ability are mediocre. This further confirms the excellent performance of our proposed model.

To further demonstrate the transfer classification results of the models for each fault category, we plot the confusion matrix for transfer diagnosis in the condition of AC→B, as shown in Figure 15. As can be seen from the comparison in the figure, the model still achieves excellent transfer diagnosis effect for C2 faults that are difficult to implement transfer classification. However, the EAFCNN model with DFAE module does not achieve a good transfer diagnosis effect for C1 and C2 faults. This further proves the excellence of our proposed SDAET model in terms of overall architecture and collocation.
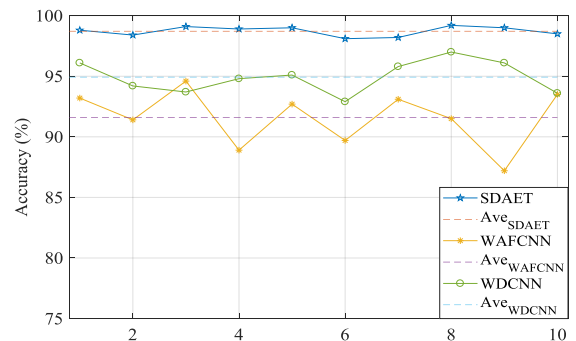

FIGURE 14. **Transfer diagnosis results of the proposed SDAET model and comparison models in the condition of AC→B.**
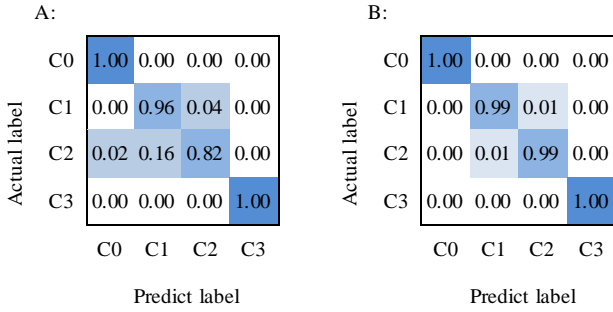
A:

B:

FIGURE 15. Confusion matrix for transfer diagnosis in the condition of AC→B. (A) EAFCNN model. (B) SDAET model.

Finally, in order to further test the diagnosis performance of the SDAET model under larger rotational speed aspan transfer and more different transfer conditions, we also carried out transfer diagnosis experiments under another four conditions. Figure 16 shows the experimental results of multiple transfer diagnosis under four transfer conditions. It can be seen from the figure that in the transfer conditions with lower speed span, namely AB→C and BC→A transfer conditions, the SDAET model achieves high transfer diagnosis accuracy, reaching about 99%. With the increase of speed span, for AB→D transfer condition, two sets of low speed data (1000r/min and 1100r/min) are completely used to transfer to high speed data (1500r/min), and the transfer performance of the proposed model is slightly reduced, only reaching about 97% of the transfer diagnosis accuracy. However, this is also a high performance to meet the requirements of industrial use. It can be seen from the above analysis that the SDAET model achieves high transfer diagnosis performance under various transfer conditions, which further proves the validity of the proposed model.
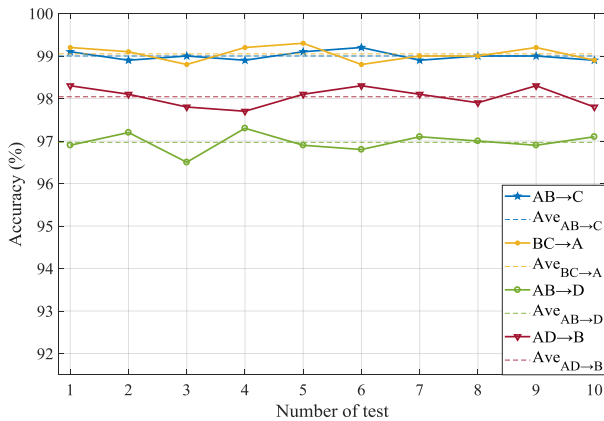

FIGURE 16. Transfer diagnosis results of the proposed SDAET model in the different transfer conditions.

VI. CONCLUSION

A siamese distinguishing feature attentional enhancement transfer (SDAET) fault diagnosis model proposed in this paper can solve the problem of migration diagnosis at variable rotational speeds. The model uses the data at any two rotational speeds as the training data, and successfully extracts the distinguishing domain invariant features at the two rotational speeds. The trained model achieves higher quality transfer diagnosis at other rotational speeds. The distinguishing feature attention enhancement network in the SDAET model also successfully and reasonably enhanced the distinguishing domain invariant features at two rotational speeds, which enabled the model to obtain better diagnostic results. All kinds of feature visualizations also further reveal the internal mechanism of the black box neural network, which is also helpful for other types of intelligent fault diagnosis algorithms.

In the future, using less tag data to achieve a more robust intelligent diagnostic model will be more worthy of research. At the same time, further research into the internal learning mechanism of neural network, to achieve more feature visualization algorithm is also very worth looking forward to. Our next research will focus on the above two aspects.

REFERENCES

[1] J. Feng, "Deep neural networks: A promising tool for fault characteristic mining and intelligent diagnosis of rotating machinery with massive data," *Mechanical Systems & Signal Processing,* vol. 72-73, pp. 303-315, 2016.

[2] H. Zhao, S. Sun, and B. Jin, "Sequential fault diagnosis based on LSTM neural network," *Ieee Access,* vol. 6, pp. 12929-12939, 2018.

[3] W. Deng, S. Zhang, H. Zhao, and X. Yang, "A novel fault diagnosis method based on integrating empirical wavelet transform and fuzzy entropy for motor bearing," *IEEE Access,* vol. 6, pp. 35042-35056, 2018.

[4] Z. Gao, C. Cecati, and S. X. Ding, "A Survey of Fault Diagnosis and Fault-Tolerant Techniques—Part I: Fault Diagnosis With Model-Based and Signal-Based Approaches," *IEEE Transactions on Industrial Electronics,* vol. 62, no. 6, pp. 3757-3767, 2015.

[5] Z. Feng, D. Zhang, and M. J. Zuo, "Adaptive mode decomposition methods and their applications in signal analysis for machinery fault diagnosis: a review with examples," *IEEE access,* vol. 5, pp. 24301-24331, 2017.

[6] X. Jiang, J. Wang, J. Shi, C. Shen, W. Huang, and Z. Zhu, "A coarse-to-fine decomposing strategy of VMD for extraction of weak repetitive transients in fault diagnosis of rotating machines," *Mechanical Systems and Signal Processing,* vol. 116, pp. 668-692, 2019.

[7] Z. An, S. Li, J. Wang, and X. Jiang, "A novel bearing intelligent fault diagnosis framework under time-varying working conditions using recurrent neural network," *ISA Transactions,* vol. 100, pp. 155-170, 2020.

[8] F. Jia, Y. Lei, J. Lin, X. Zhou, and N. Lu, "Deep neural networks: A promising tool for fault characteristic mining and intelligent diagnosis of rotating machinery with massive data," *Mechanical Systems and Signal Processing,* vol. 72, pp. 303-315, 2016.

[9] J. Korbicz, "Artificial neural networks in fault diagnosis of dynamical systems." pp. 449-449.

[10] Y. Lei, F. Jia, J. Lin, S. Xing, and S. X. Ding, "An Intelligent Fault Diagnosis Method Using Unsupervised Feature Learning Towards Mechanical Big Data," *IEEE Transactions on Industrial Electronics,* vol. 63, no. 5, pp. 3137-3147, 2016.

[11] S. Lu, Q. He, and J. Zhao, "Bearing fault diagnosis of a permanent magnet synchronous motor via a fast and online order analysis method in an embedded system," *Mechanical Systems and Signal Processing,* vol. 113, pp. 36-49, 2017.

[12] K. Xu, S. Li, X. Jiang, J. Lu, T. Yu, and R. Li, "A novel transfer diagnosis method under unbalanced sample based on discrete-peak joint attention enhancement mechanism," *Knowledge-Based Systems*, vol. 212, pp. 106645, 01/05, 2021.

[13] F. Zhou, S. Yang, H. Fujita, D. Chen, and C. Wen, "Deep learning fault diagnosis method based on global optimization GAN for unbalanced data," *Knowledge-Based Systems*, vol. 187, pp. 104837, 2020.

[14] W. Zhang, G. Peng, C. Li, Y. Chen, and Z. Zhang, "A New Deep Learning Model for Fault Diagnosis with Good Anti-Noise and Domain Adaptation Ability on Raw Vibration Signals," *Sensors*, vol. 17, no. 2, pp. 425, 2017.

[15] R. Li, S. Li, K. Xu, J. Lu, G. Teng, and J. Du, "Deep domain adaptation with adversarial idea and coral alignment for transfer fault diagnosis of rolling bearing," *Measurement Science and Technology*, vol. 32, no. 9, pp. 094009, 2021/06/08, 2021.

[16] W. Qian, S. Li, P. Yi, and K. Zhang, "A novel transfer learning method for robust fault diagnosis of rotating machines under variable working conditions," *Measurement*, vol. 138, pp. 514-525, 2019/05/01/, 2019.

[17] M. Long, Y. Cao, J. Wang, and M. Jordan, "Learning transferable features with deep adaptation networks." pp. 97-105.

[18] J. Jiao, M. Zhao, and J. Lin, "Unsupervised adversarial adaptation network for intelligent fault diagnosis," *IEEE Transactions on Industrial Electronics*, vol. 67, no. 11, pp. 9904-9913, 2019.

[19] M. Ghifary, W. B. Kleijn, M. Zhang, D. Balduzzi, and W. Li, "Deep reconstruction-classification networks for unsupervised domain adaptation." pp. 597-613.

[20] C. Che, H. Wang, X. Ni, and Q. Fu, "Domain adaptive deep belief network for rolling bearing fault diagnosis," *Computers & Industrial Engineering*, vol. 143, pp. 106427, 2020.

[21] B. Yang, Y. Lei, F. Jia, N. Li, and Z. Du, "A polynomial kernel induced distance metric to improve deep transfer learning for fault diagnosis of machines," *IEEE Transactions on Industrial Electronics*, vol. 67, no. 11, pp. 9747-9757, 2019.

[22] X. Li, Y. Hu, J. Zheng, M. Li, and W. Ma, "Central moment discrepancy based domain adaptation for intelligent bearing fault diagnosis," *Neurocomputing*, vol. 429, pp. 12-24, 2021/03/14/, 2021.

[23] Q. Qian, Y. Qin, Y. Wang, and F. Liu, "A new deep transfer learning network based on convolutional auto-encoder for mechanical fault diagnosis," *Measurement*, vol. 178, pp. 109352, 2021/06/01/, 2021.

[24] T. Han, C. Liu, W. Yang, and D. Jiang, "A novel adversarial learning framework in deep convolutional neural network for intelligent diagnosis of mechanical faults," *Knowledge-Based Systems*, vol. 165, pp. 474-487, 2019/02/01/, 2019.

[25] J. Jiao, M. Zhao, J. Lin, and K. Liang, "Residual joint adaptation adversarial network for intelligent transfer fault diagnosis," *Mechanical Systems and Signal Processing*, vol. 145, pp. 106962, 2020/11/01/, 2020.

[26] Z. Chen, G. He, J. Li, Y. Liao, K. Gryllias, and W. Li, "Domain Adversarial Transfer Network for Cross-Domain Fault Diagnosis of Rotary Machinery," *IEEE Transactions on Instrumentation and Measurement*, vol. 69, no. 11, pp. 8702-8712, 2020.

[27] E. Alves, P. Machado, T. Massoni, and M. Kim, "Prioritizing test cases for early detection of refactoring faults," *Software Testing, Verification and Reliability*, vol. 26, pp. n/a-n/a, 03/01, 2016.

[28] Y. Gu, L. Zeng, and G. Qiu, "Bearing fault diagnosis with varying conditions using angular domain resampling technology, SDP and DCNN," *Measurement*, vol. 156, pp. 107616, 2020/05/01/, 2020.

[29] A. Zhang, S. Li, Y. Cui, W. Yang, R. Dong, and J. Hu, "Limited Data Rolling Bearing Fault Diagnosis With Few-Shot Learning," *IEEE Access*, vol. 7, pp. 110895-110904, 2019.

[30] X. Li, W. Zhang, and Q. Ding, "Understanding and improving deep learning-based rolling bearing fault diagnosis with attention mechanism," *Signal processing*, vol. 161, no. AUG., pp. 136-154, 2019.

[31] S. Ioffe, and C. Szegedy, "Batch Normalization: Accelerating Deep Network Training by Reducing Internal Covariate Shift," *international conference on machine learning*, pp. 448-456, 2015.

[32] K. Xu, S. Li, R. Li, J. Lu, M. Zeng, X. Li, J. Du, and Y. Wang, "Cross-domain intelligent diagnostic network based on enhanced attention features and characteristics visualization," *Measurement Science and Technology*, vol. 32, no. 11, pp. 114009, 2021/08/12, 2021.

[33] S. Chopra, R. Hadsell, and Y. Lecun, "Learning a similarity metric discriminatively, with application to face verification." pp. 539-546.

[34] D. P. Kingma, and J. Ba, "Adam: A Method for Stochastic Optimization," *international conference on learning representations*, 2015.

[35] Wade, A., Smith, Robert, B., and Randall, "Rolling element bearing diagnostics using the Case Western Reserve University data: A benchmark study," *Mechanical Systems and Signal Processing*, vol. 64-65, pp. 100-131, 2015.

[36] Z. An, S. Li, J. Wang, Y. Xin, and K. Xu, "Generalization of deep neural network for bearing fault diagnosis under different working conditions using multiple kernel method," *Neurocomputing*, 2019.